ADVANCED MATERIALS INTERFACES
www.advmatinterfaces.de

In-Depth NMR Investigation of the Magnetic Hardening in Co Thin Films Induced by the Interface with Molecular Layers

Mattia Benini, Giuseppe Allodi,* Alessandro Surpi, Alberto Riminucci, Ko-Wei Lin, Samuele Sanna, Valentin Alek Dediu,* and Ilaria Bergenti**

The hybridization of the surface orbitals of thin ferromagnetic layers with molecular orbitals represents a soft but efficient technology that is able to induce in ferromagnetic component radical modifications of the key magnetic parameters, such as magnetization, magnetic anisotropy, and others. These effects are investigated in 7 nm thick polycrystalline Co films interfaced with C_{60} and Gaq_3 molecular layers by combining ^{59}Co Ferromagnetic nuclear resonance spectroscopy (FNR) and magneto-optic kerr effect (MOKE) techniques. It is demonstrated that the surface hybridization produces a significant magnetic hardening with respect to a reference Co/Al system and that the molecule-induced effects modify the magnetic properties of entire Co layer, propagating for several nm from the interface. The FNR spectroscopy also reveals a reconstruction of the magnetic environment at the cobalt surface, whose observation in polycrystalline films is especially intriguing. The results shed new and unexpected light on the interfacial physics in such systems, whose understanding necessitates further experimental and theoretical research.

1. Introduction

The interfaces between ferromagnetic thin films and chemisorbed molecular layers exhibit a variety of interesting phenomena.[1] The active investigation of these so-called spinterfaces[2,3] started with the advancement of molecular or organic-based spintronic devices, and initially it was strongly focused on the modifications of molecular layers induced by the vicinity of a ferromagnetic material. The spin-dependent broadening of the localized HOMO-LUMO electronic levels[2,4,5] and related spin filtering effects[6–8] had a key role in the understanding of organic spin valves and other organic-based spintronic devices. Also, the establishment of detectable spin polarization in vicinal molecules has opened a new investigation field related to the propagation of the magnetic order in molecular materials. This results in the presence of magnetic dichroic signals on the molecule-constituting elements[9] or in the formation of non-trivial oscillations of the spin order as a function of the energy of molecular electronic states.[10,11]

On the other hand, the interfacial proximity effects are likely to modify also the ferromagnetic counterpart. The first observation of this was reported in 2013, when a new 2D magnetic layer proved to form at the interface between metallic cobalt and an organometallic molecule (zinc methyl phenalenyl).[12] The new magnetic phase was characterized at low temperatures by a coercive field enhanced by over an order of magnitude with respect to the underneath cobalt layer. Such magnetic hardening effects have been later observed for various other spinterfaces,[13–16] breaking the ground for a new research field. Among these, the Co/C_{60} interface has attracted major interest and exhibited a number of promising results, such as the considerable enhancement of the in-plane magnetic anisotropy in polycrystalline cobalt layers,[13,17] or even the in-plane to out-of-plane rotation of the easy axis for ultrathin epitaxial Co films.[14] Moreover, the interfacial hybridization effects were found to induce ferromagnetic order in copper-based Cu/C_{60} multilayered structures, opening the extraordinary possibility to transform non-magnetic in ferromagnetic materials.[18] One of the main questions arising in this context is whether the molecule-induced modifications are localized near the interface or they

M. Benini, A. Surpi, A. Riminucci, V. A. Dediu, I. Bergenti
CNR-ISMN
Via Piero Gobetti 101, Bologna 40129, Italy
E-mail: mattia.benini@ismn.cnr.it; valentin.dediu@cnr.it; ilaria.bergenti@cnr.it
M. Benini, S. Sanna
Department of Physics and Astronomy
A. Righi
University of Bologna
via Berti Pichat 6-2, Bologna I-40127, Italy
G. Allodi
Department of Mathematical
Physical and Computer Sciences
University of Parma
Parco Area delle Scienze, 7/A Parma 43124, Italy
E-mail: giuseppe.allodi@unipr.it
K.-W. Lin
Department of Materials Science and Engineering
National Chung Hsing University
145 Xingda Rd., Taichung City 402, Taiwan

DOI: 10.1002/admi.202201394

can extend to a significant portion of the ferromagnet. In this paper, we mainly address this question and investigate it by employing a detailed ^{59}Co nuclear magnetic resonance (NMR) study of Co/C_{60} and Co/Gaq_3 spinterface-based bilayers.

The resonance of nuclei of magnetic ions in ferromagnetic materials, also referred to as zero-field NMR or ferromagnetic nuclear resonance (FNR),[19] can be excited and detected in zero external applied field.[20,21] In such systems the nuclear spins experience a spontaneous hyperfine field (HF) generated locally by the ordered electronic magnetic moments.[21–23] As a consequence of this, the radiofrequency (rf) field experienced by the nuclei is enhanced by the electronic magnetic susceptibility of the sample. The material characterization provided by FNR is based on the zero-field NMR spectrum, the rf enhancement of the resonance, as well as possible correlations between the spectral response and inhomogeneities in the enhancement factor. The distribution of the hyperfine fields at the nuclear probe, directly proportional to the NMR spectral density, yields valuable information about the electronic state of the magnetic ion and the local structure of its surrounding. Moreover, the nanoscale magnetic properties of the material (e.g., the magnetic domain texture) are probed through the enhancement factor, arising from the coupling of the HF to the electronic magnetic moment and the coupling of the latter to the radio-frequency field in the sample coil. In a ferromagnet, the driving oscillating field at the nucleus and the oscillating magnetic flux in the pick-up coil are essentially due to the transverse oscillatory modulation of the hyperfine field, and to the oscillation of the hyperfine-coupled electronic magnetization, respectively.[19] As a consequence, both the excitation and the response of the nuclear resonance are amplified by the enhancement factor η proportional to the transverse magnetic susceptibility, and hence inversely proportional to the magnetic anisotropy. Over the years, FNR has proved to be a powerful technique for the characterization of magnetic multilayers[24,25] and alloys.[26] More recently, it has also been successfully employed for the investigation of the interface (spinterface) quality in hybrid spintronic devices with organic molecules placed between two ferromagnetic electrodes.[27,28]

In this work, we investigated the ^{59}Co FNR response of 7 nm polycrystalline cobalt films interfaced with two different molecules: Buckminster-fullerene (C_{60}) and Tris(8-hydroxyquinolinato)gallium (Gaq_3). The surface morphology of the starting cobalt layer was probed by ex-situ AFM microscopy, while its crystallinity and the quality of the Co/molecule interface were studied by cross-section transmission electron microscopy (TEM). The magnetization dynamics were additionally studied from hysteresis loops obtained from longitudinal magneto-optic Kerr effect (L-MOKE). To evidence the interface-induced effects, the data were benchmarked to those of a reference 7 nm-thick Co thin film capped with Al. The capping layer is necessary to avoid the formation of cobalt oxides, able to promote non-trivial magnetic interactions with the underlying cobalt. The choice of aluminum as a capping layer is due to its low atomic number and its low intermixing when deposited over a Co surface, a property that was successfully employed previously.[29,30] Moreover, it has been shown that even 2 nm of Al protect the cobalt layer from oxidation for at least 10^4 h.[31] Finally, the 7 nm thickness for Co films was selected as the lowest thickness enabling significant FNR signals, while emphasizing the role of the interface.

2. Structural Characterizations

The quality of the interface between the ferromagnetic layer and organic molecules plays a major role in the definition of the overall properties of investigated bilayers. To guarantee the highest quality of the cobalt layer, we employed terraced Al_2O_3(0001) substrates. For bare cobalt films (Al_2O_3(0001)// Co(7 nm)), AFM microscopy shows a flat surface (**Figure 1**a) with RMS roughness of (0.3 ± 0.1) nm and clear evidence of the substrate terraces. The surface features are typical for a polycrystalline sample, showing grains with average lateral size of (9.8 ± 0.5) nm. The deposition of a 25 nm thick organic layer guarantees the full coverage of the Co layer, preventing it from oxidation and does not strongly enhance the surface roughness, as shown in Figure 1b,c) for the Gaq_3Co (Al_2O_3(0001)// Co(7 nm)/Gaq_3(25 nm)) and the C_{60}Co (Al_2O_3(0001)//Co(7 nm)/ C_{60}(25 nm)) samples. Similar roughness was observed also for the reference sample, AlCo (Al_2O_3(0001)//Co(7 nm)/Al(8 nm)). The microstructure of the Co layer was investigated by cross-section TEM on an on-purpose fabricated 10 nm thick Co film capped with 25 nm C_{60} (see **Figure 2**). The image shows randomly oriented nanometer-sized grains in the fcc and hcp phases, as deduced from the crystalline interplanar distances.

3. FNR and L-MOKE Investigation

The ^{59}Co FNR characterization of the samples was carried out at 77 K in zero dc field by a standard procedure, using the same radiofrequency (rf) circuitry and sample coil for all the samples. rf pulses of constant duration τ were used to excite 90°-90° nuclear spin echoes, at frequencies ν from 190 to 240 MHz (an interval comprising practically all the ^{59}Co spectral intensity) and changing the power P_{rf} of the driving rf pulses in the range of 14–40 dBm.

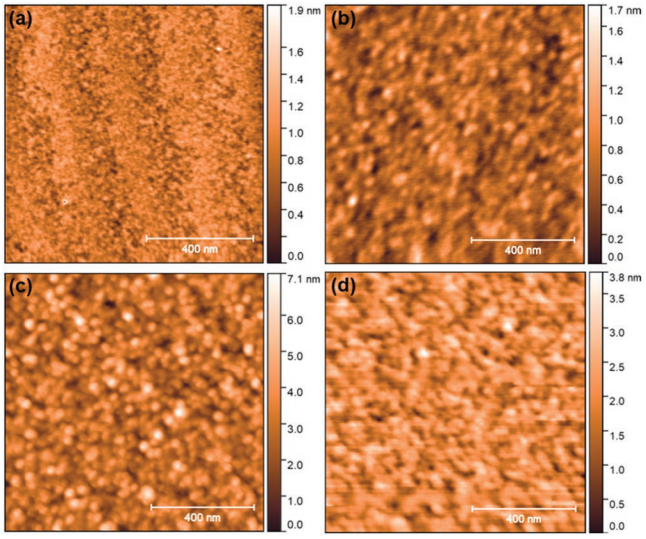

Figure 1. One micrometer wide AFM images of a) a bare Co(7 nm) surface, showing a granular structure and also a substrate-induced terraces; RMS of (0.3 ± 0.1) nm. b) The AlCo surface, RMS of (0.3 ± 0.1) nm. c) The C_{60}Co surface, RMS of (0.9 ± 0.1) nm. d) The Gaq_3Co surface, RMS of (0.4 ± 0.1) nm.

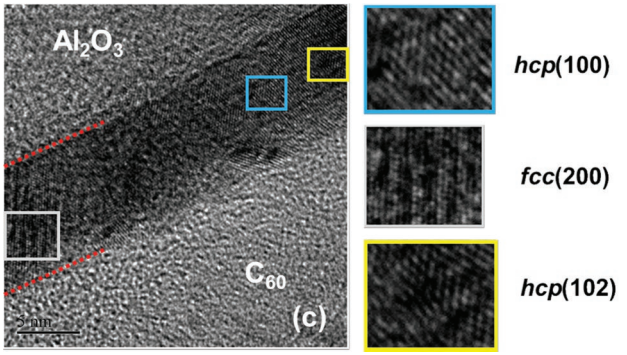

Figure 2. CROSS-TEM image of a 10 nm Co ultra-thin film capped with 25 nm C_{60}. Colored squares identify some examples of regions with defined crystallinity.

The rf power scan accounts for the distribution of excitation conditions, originating from the distribution of enhancement factors η in the material. As introduced above, in a ferromagnetic material the applied rf field excites the nuclear spins indirectly through the rotation of the electronic magnetic moment and its hyperfine coupling to the nuclear spins, so that the effective *ac* field $B_1^{(eff)}$ at the nucleus is essentially the oscillating hyperfine field. Note that the electronic magnetic moments respond adiabatically, since the used excitation frequencies are far from any magnetic electronic resonance.[19]

As a consequence of this, $B_1^{(eff)}$ is enhanced with respect to the driving rf field H_{rf} in the sample coil by the enhancement factor η, ranging in ferromagnets between 10^2 and 10^4.[19,22] In polycrystalline samples the enhancement factor η is essentially inhomogeneous, due to the presence of different domain orientations relative to $\mathbf{H}_{rf}$, demagnetization fields, and different micromagnetic structures. In our experiments, by applying a given rf power (hence, a given $H_{rf} \propto \sqrt{P_{rf}}$), we select the population of nuclei resonating at the optimum nutation angle $\theta = \pi/2 = \eta\gamma H_{rf}\tau$ (where γ is the nuclear gyromagnetic ratio and τ is the rf pulse duration) and $\eta = \pi/(2\gamma H_{rf}\tau)$. Nuclei with significantly different η, hence nutating by either $\theta \gg \pi/2$ or $\theta \ll \pi/2$ under an rf pulse, are not properly excited and their contribution to the NMR signal is negligible.

The 2D ^{59}Co FNR spectra as a function of frequency and P_{rf} for the C_{60}Co and Gaq_3Co samples, as well as for the reference Co-Al, are shown in **Figure 3** as 3D maps (Figure 3a–c) and 2D contour colormaps (Figure 3d–f). These spectra, having most of their spectral weight in the 210–230 MHz range, are typical for polycrystalline cobalt samples.[19,32] The AlCo and C_{60}Co films exhibit maximum intensity at ≈222 MHz, closer to the ^{59}Co resonance reported for *hcp* cobalt, while the main peak of Gaq_3Co is found at ≈215 MHz, close the ^{59}Co peak of the *fcc* phase.[16] It is unlikely that these samples are characterized by different microstructures since for each sample the growth of the Co pristine layer has been done during the same deposition, ensuring the same thickness, morphology, and crystalline composition. Even though the hybridization with molecules can lead to surface reconstruction of Co and other *3d* metals,[33,34] it is generally not expected that molecules can induce in-depth modifications of the Co microstructure (see more details in the discussion).[1,13,15,35] The apparent *hcp*/*fcc* change may result from the specific modification of the hyperfine fields at the Co surface hybridized with molecules and inducing these characteristic frequencies.

The comparison of the colormaps of Figure 3d–f of the three samples, clearly shows an increase in the optimum $P_{rf}^{(opt)}$ needed to obtain the maximum spin-echo signal moving

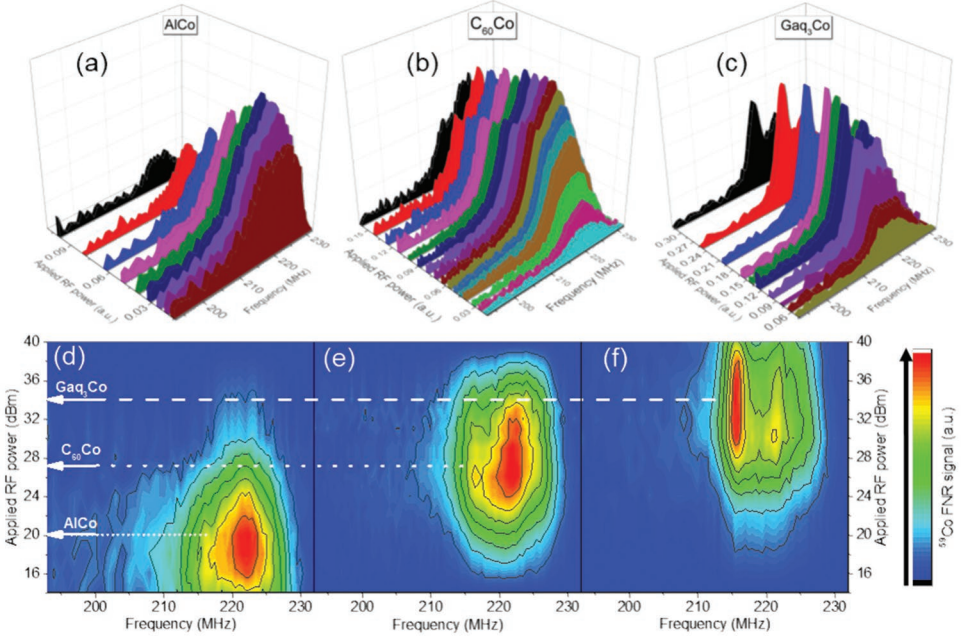

Figure 3. a–c) 3D contour plots showing the ^{59}Co FNR signal as a function of the frequency and applied rf power for AlCo (left), C_{60}Co (center), and Gaq_3Co (right) samples. The colors attributed to each spectrum is merely a guide for the eye. d–f) 2D contour colormaps (blue: lowest value, red: highest value) of AlCo (left), C_{60}Co (center) and Gaq_3Co (right) samples. The white arrow indicates the position of the global maximum measured spin-echo signal.

from AlCo to C_{60}Co and further to Gaq_3Co. This corresponds to a decrease in the mean enhancement factor $\overline{\eta} \propto 1/\sqrt{P_{rf}^{(opt)}}$. Within the adiabatic response of the electronic moments to the rf field,[21,25] η is proportional to the dc transverse magnetic susceptibility,[19] in its turn inversely proportional to the combination of the magneto-crystalline anisotropy, the demagnetization and the applied field (if present). This is accounted for by the effective restoring field H_R, defined as the equivalent magnetic field exerting a torque on the electronic spins tilted from their equilibrium direction.[19,21] Therefore, the progressive shift to higher optimum excitation power, hence to higher $H_R \propto \sqrt{P_{rf}^{(opt)}}$, witnesses an increased magnetic hardness in C_{60}Co and even more markedly in Gaq_3Co with respect to capped cobalt layer (AlCo).

In the 2D scans of Figure 3a–f, it is clear that the spectral shapes of each sample are practically independent of H_{rf}. The lack of noticeable correlations between resonance frequency and applied power provides strong evidence in favor of high structural homogeneity in the magnetic layer. The existence of segregated structural phases or exchange-decoupled magnetic domains would correspond to a power-dependent shape of the frequency spectrum. Indeed, a specific magnetic phase would be excited preferentially by tuning H_{rf},[36] which is contrary to our experimental evidences.

The same conclusion can be drawn by examining the spectral dependence of the optimum rf excitation $H_{rf}^{(opt)}(\nu) \propto \sqrt{P_{rf}^{(opt)}(\nu)}$ of the C_{60}Co and Gaq_3Co samples, where $P_{rf}^{(opt)}(\nu)$ is the applied power leading to the maximum spin-echo signal. It is determined for each frequency from a fit of the NMR signal amplitude $A(\nu,P_{rf})$ to a Gaussian function in $\log(P_{rf})$.[19] For a more clear and accurate elucidation of the hardening effects, we analyze the frequency dependence of ratio $R = H_{rf}^{(opt)}(X)/H_{rf}^{(opt)}(Al)$, where X stands for either C_{60} of Gaq_3 based samples. In **Figure 4**a the ratio R is plotted versus frequency over the 210–230 MHz range, where the spin-echo intensity allows for a reliable fitting. The main feature clearly emerging from Figure 4a, is that C_{60}Co and Gaq_3Co are magnetically harder than the reference AlCo film by factors as high as R = 3 and R = 5, respectively.

Importantly, the figure shows a substantially flat R, whose residual modulation $\Delta R/R \leq 30\%$ can be deemed small compared to the typical $H_{rf}^{(opt)}(\nu)$ profiles encountered in inhomogeneous cobalt layers and showing variations through the spectrum by nearly an order of magnitude.[21,32] This additionally confirms that the investigated C_{60}Co and Gaq_3Co films are homogeneous on a mesoscopic scale. Finally, note that the use of ratios $R = H_{rf}^{(opt)}(X)/H_{rf}^{(opt)}(Al)$ (X = C_{60}, Gaq_3) allows for eliminating all possible spurious contributions in the frequency response of the apparatus.

The magnetic hardening induced by molecular overlayers was confirmed by ex situ measurements of L-MOKE hysteresis loops at the same temperature of 77 K in external field H applied along the same direction as H_{rf} field (Figure 4b). As mentioned in the introduction MOKE technique is one of the most standard methods to investigate such interfaces. From these hysteresis loops, the coercive fields are determined as $\mu_0 H_C$ = (5.0 ± 3) mT, (9.6 ± 0.4) mT, and (14.1 ± 0.4) mT in AlCo, C_{60}Co and Gaq_3Co, corresponding to 1.9- and 2.8-times enhancement of the coercive fields, respectively.

Both FNR and MOKE techniques consistently indicate the same trend for magnetic hardening in C_{60}Co and Gaq_3Co samples. A quantitative comparison between the two techniques is not straightforward. The FNR restoring fields can be directly related to anisotropy field or coercive fields detected by MOKE only in particular cases and geometries, [21] like for example a single domain uniaxial particle. This is not the case in our polycrystalline samples. Moreover, the situation is complicated by the dissimilar magnetization dynamics generated in the two cases: high-frequency reversible modulation in FNR, and pseudo-static irreversible modification of magnetization in MOKE.

Importantly, the shifts of the optimal P_{rf} of the molecule-covered cobalt layer to higher powers, an effect emphasized in Figure 4a, clearly indicates that the observed hardening propagates to the whole thickness of the investigated cobalt layer. Indeed, the optimal power for the excitation of AlCo does not produce measurable rotation of the electronic magnetic moment in C_{60}Co and Gaq_3Co.

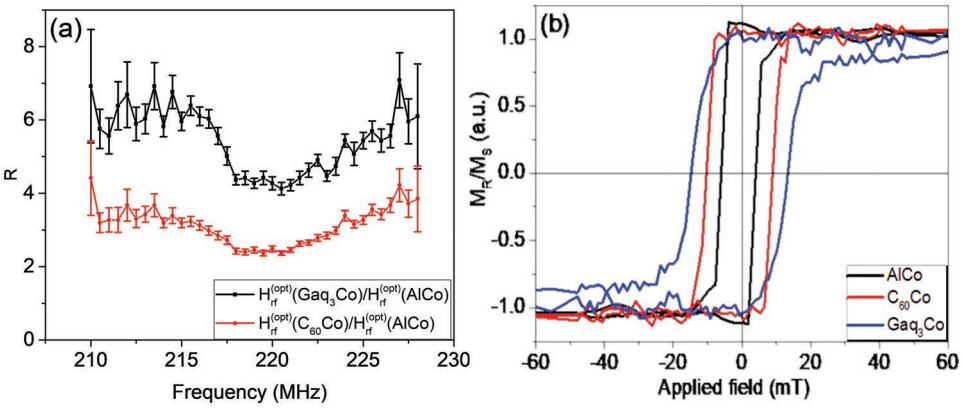

Figure 4. a) Ratio R of the optimal rf field of the Co/molecule systems ($H_{rf}^{(opt)}$ (X)) divided by the optimal rf field of the reference sample ($H_{rf}^{(opt)}$ (Al)), proportional to the ratio between the mean enhancement factor of the Co/molecule system and the corresponding of the reference sample. b) L-MOKE normalized hysteresis loops at 77 K for Gaq_3-Co and C_{60}-Co. The applied field direction is the same as the rf field in NMR experiments.

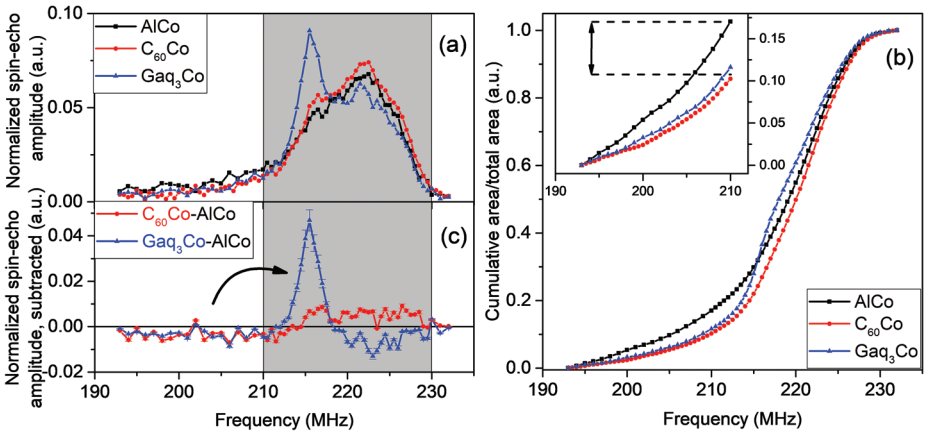

Figure 5. a) ^{59}Co Normalized FNR spectra of each sample (shaded region corresponds to bulk Co). b) Normalized cumulative spectral area of each sample. Inset: normalized cumulative spectral area for frequencies below 210 MHz, highlighting (double arrow) the differences between the overall low-frequency contribution to the spectral area from the low frequency shoulder. c) The normalized spectra of C_{60}Co (red) and Gaq_3Co (blue) subtracted by that of Al-Co, showing a minor negative contribution in the low frequency and a sample-dependent positive contribution in the bulk (shaded) region.

The analysis of the spectral shape of FNR signals allows nevertheless extraction of additional details of the magnetic order unavailable to MOKE characterizations. It is possible to gain insight into the interfacial properties of the Co films with their non-magnetic overlayers, by comparing the spectral density of ^{59}Co nuclei $n(\nu)$ in various samples (**Figure 5**a). This last quantity is calculated at each frequency ν, as the maximum spectral amplitude $\frac{A(\nu, P_{rf}^{(opt)})}{\overline{\eta}(\nu) \propto 1/\sqrt{P_{rf}^{(opt)}(\nu)}}$ and, subsequently, normalized to the full spectral area. Thus $n(\nu)$ represents the fraction of resonating ^{59}Co nuclei per unit frequency. Our normalized spectra clearly show a low-frequency tail extending well below 210 MHz, i.e., below the frequency range assigned to the bulk (shaded area). The fraction of nuclei resonating at such low frequencies (i.e., the area under the $n(\nu)$ curves for $\nu \leq 210$ MHz) is estimated as (17 ± 2) % in AlCo. This is significantly higher than in C_{60}Co and Gaq_3Co, which exhibit a low-frequency fraction of (10 ± 1) % and (12 ± 1) %, respectively. The complementary transfer of spectral weight to a higher frequency in C_{60}Co and Gaq_3Co is also apparent in Figure 5b, showing the cumulative spectral distributions of nuclei of the three samples, and in Figure 5c, showing the difference in the spectral density of C_{60}Co and Gaq_3Co with respect to the reference $n(\nu)$ of AlCo. This low-frequency shoulder of the spectrum is associated in polycrystalline cobalt with Co atoms in a defective environment relative to the bulk, as for instance grain boundaries,[24] interfaces with non-magnetic species like copper or aluminum[25–27,37] or other. Within this interpretation, the spectral weight transfer in C_{60}Co and Gaq_3Co indicates a reduced defectiveness at the interface with the molecular layer. From our data, the molecule-induced electronic modification involves ≈5% of Co atoms or a thickness of ≈3–4 Å close to the interface, effectively corresponding to a monolayer. This indicates a modification of the magnetic order at the surface of cobalt/molecule structures, corresponding to a kind of magnetic reconstruction (see the discussion part).

Note that some residual low-frequency signal fraction in both C_{60}Co and Gaq_3Co, indicates that at least part of the disorder is independent of the interface and can be tentatively attributed to Co atoms in grain boundaries,[32] likely present in polycrystalline samples. Also, the difference between AlCo and molecular-based samples can be partly due to the diffusion of aluminum in cobalt, producing up to 0.8 nm intermixed Co-Al interfacial layers,[29,30,38] and thus inducing additional defectiveness at the Co surface with respect to an ideal Co surface environment. Nevertheless, the above consideration alone cannot explain the strong, molecule-dependent differences in the spectral shapes of Co/C_{60} and Co/Gaq_3.

4. Conclusion

Our paper presents the first-time detection by FNR spectroscopy of the magnetic hardening in two Co/Molecule systems, namely in Co/C_{60} and in Co/Gaq_3 bilayers. The hardening effect is confirmed by more standard MOKE characterizations, linking our results to previously published data. Noteworthily, the application of FNR technique allowed us to unravel previously unknown properties of Co/Molecule spinterfaces and sheds new light on already debated problems.

Considering the FNR measurements, the hardening was defined through the increase of the optimal applied rf power (Figure 3) and from the restoring field ratio R in Figure 4a. Figure 3, and especially the 2D contour colormaps (Figure 3d–f), firmly answer the key question advanced in the introduction of this paper, namely how deep does the interfacial-induced hardening penetrate in the Co layer. The clear shift of applied power maps with minor broadening and deformation indicates that the induced hardening characterizes the whole 7 nm thick Co layer. We believe that this information, even though perceivable from standard magnetization measurements, such as MOKE or SQUID, is for the first time undeniably ascertained.

On the other hand, the large majority of ^{59}Co nuclei resonating at frequencies appropriate for bulk metallic cobalt[21,22,25] and the absence of long-range spatial segregations indicate that

the sizable modification of the magnetic susceptibility, though extended through the whole Co layer, is not accompanied by large structural or electronic modifications inside it. Consequently, the magnetic hardening must be an effect of the interface, propagating to length scales of several nanometers.

Finally, Figure 4 allows to quantify the modification of the magnetic anisotropy in interface-engineered cobalt layers: the restoring field and hence the magnetic stiffness[19,32] is noticeably enhanced by a factor of 3 in Co/C_{60} and by factor of 5 in Co/Gaq_3.

The interface-induced effects are additionally emphasized in the spectral weight transfer detected for the NMR spectra. The transfer from the low-frequency tail (below 210 MHz) to higher frequencies characteristic for the bulk cobalt was clearly observed for the two molecule-hybridized films with respect to the reference sample and involved ≈5–7% of ^{59}Co nuclei (Figure 5b,c). Moreover, the spectrum of Gaq_3Co features the appearance of a relatively sharp peak at 215 MHz representing ≈7–8% of cobalt atoms, generated by the spectral weight shift from AlCo (see Figure 5c).

As discussed above in the experimental part, the partial suppression of the low-frequency spectral component indicates a reduced defectiveness of the magnetic structure of the cobalt surface in Co/Molecule systems. This effectively corresponds to a new kind of magnetic reconstruction of the surface. Indeed, as clear from Figure 5c the surface Co atoms in Co/C_{60} and Co/Gaq_3 are characterized by a higher fraction of cobalt atoms resonating at bulk-like frequencies of Co than those of the reference sample.

The further spectral differences between the two molecular cases explicitly emphasize the role of molecules in this reconstruction effect. Both C_{60} and Gaq_3 molecules are covalently bound to a fraction of surface cobalt atoms and the resulting *p-d* hybridization modifies the magnetic moment of respective atoms. This generates surface magnetic structures strongly dependent on the molecular size, shape, and symmetry.[39,40]

It is important to mention that several experimental and theoretical papers claimed the possibility of a structural reconstruction of Co[34] and Ni[33,41] surfaces interfaced with C_{60} molecules. It has been predicted and observed that the molecules induce metal vacancies by substituting 7 metal atoms and lying nested into the first Co layer. We note nevertheless that such surface reconstruction requires special post-annealing procedures at ≈550–600 K that was intentionally avoided in our fabrication methods.

Moving now to the hardening effects, the role of *p-d* hybridization between molecules and thin *3d* magnetic films has been emphasized in a number of experimental and theoretical works. At the microscopic level extensive DFT calculations[12,14,39,42] unraveled the geometry and the energetics of the interaction between molecules and surface atoms. It was shown that the interfacial hybridization results in major modification of some magnetic parameters of the *3d* metal atoms bound to selected atoms in the molecules. Among these, we would like to mention a substantial decrease in the magnetic moments (up to 30–40%[35,39]) accompanied by major modifications of the in-plane exchange interactions between surface atoms.[42] All the models unequivocally point to the enhanced magnetic anisotropy, calculated by summing the contributions from individual atoms. Noteworthily, this enhancement is strongly confined in the last monolayer of the magnetic surface, with minor extension to the second monolayer.[14,15]

The physical meaning of the processes induced by *p-d* bonding can be better understood on the basis of a stronger hybridization of molecular orbitals with out-of-plane *3d* orbitals than with in-plane ones.[14] In our opinion, this can be linked to the Bruno's model of the magnetic anisotropy in ultrathin layers of *3d* magnets,[43] by a hybridization-induced variation of the parameter Δ, associated with the energy difference between out of plane (yz, zx, $3z^2$-r^2) and in plane (xy, x^2-y^2) orbitals.

Note that the above models and considerations promote as a key mechanism the purely electronic effect of the molecules on surface cobalt atoms via the modification of their d-orbitals, responsible in turn for the modification of all the magnetic properties in ferromagnetic metal.

It is clear that the described above theoretical models and calculations can explain well the modifications of magnetic anisotropy in a few monolayer thick films, and more generally must be taken into account for analyzing also the effects in thicker films. We believe nevertheless that for the latter case additional physics must be considered: indeed, in this paper we present data on strong variations of magnetic anisotropy across 7 nm thick films of Co, approximately exceeding 20 monolayers and with magnetic hardening expanding to scales well beyond those predicted in the discussed models.

A possible scenario could be represented by an unusually strong pinning of domain walls by the surface hybridized layer of cobalt. The magnetic configuration of the uppermost Co atoms, modified by the interaction with the molecules, can act as an obstacle to domain wall motion. Given that the thickness of our cobalt layers is comparable to its characteristic exchange length of a few nanometers,[44] the interfacial layer affects the susceptibility of the entire magnetic system, resulting in the induced hardening of the bulk. The role of pinning effects in such systems has been considered also by other authors for both epitaxial[15] and polycrystalline cases.[17]

Furthermore, we cannot exclude at this stage possible variations of the microscopic magnetic parameters in the bulk of the cobalt layer. For example, the modification of *d*-orbitals at the interface may propagate to the bulk via the *s-d* hybridization in Co, resulting in a modification of the spin polarization (SP) of the delocalized *s* electrons, and hence in a change of the hyperfine fields. Note that the conduction electrons account for ≈10% of the HF,[45] so that our FNR results exclude a strong modification of the SP, which would result in a measurable shift of the resonance frequencies. Yet, taking as an example a variation of about one tenth of the SP, which is critically important for spintronic devices, would cause a frequency shift of the order of 1%, hardly detectable in our experiment. We believe this issue requires dedicated research in properly tailored spintronic devices.

In conclusion, the ^{59}Co zero-field NMR characterization of Co/C_{60}, Co/Gaq_3, and reference Co/Al samples has proven to be an efficient technique for the investigation of the molecule-induced magnetic hardening in ferromagnetic layers confirmed in parallel by L-MOKE measurements. The increase of the optimal applied rf power and the overall increase of the restoring fields unequivocally demonstrates that magnetic

anisotropy is modified on several nanometer scales. The modification is dependent on the molecule and corresponds to a 5- and 3-times enhancement of the restoring fields in Co/Gaq_3 and Co/C_{60} systems respectively, in comparison with the reference cobalt layer. FNR spectroscopy revealed additionally a molecule-dependent reconstruction of the local magnetic environment at the Co surface, induced by hybridization. The investigated interface hybridization proves to be a powerful and versatile technology for the design and fabrication of nm-scale thick films for magnetic and spintronic applications with tailored on-demand magnetic parameters.

5. Experimental Section

Sample Preparation: The samples were grown in an ultra-high vacuum environment on Al_2O_3(0001) single-crystal substrates. Deposition chambers were connected under high vacuum, so that samples can be transferred without breaking the UHV conditions. The pristine 7 nm – thick cobalt layers were grown by e-beam evaporation, with a deposition rate of 0.03 Å sec^{-1}, during the same evaporation on different substrates. These latter were kept at room temperature with base pressure of $4*10^{-10}$ mbar. The molecular layers (thickness of 25 nm) and the Al layer (8 nm thickness) were then deposited from effusion cells in a chamber with a base pressure of $1*10^{-8}$ mbar, keeping the Co layer at RT. Deposition rate was 0.15 Å sec^{-1} for C_{60}, 0.25 Å sec^{-1} for Gaq_3 and 0.1 Å sec^{-1} for Al.

Structural Investigation: Surface morphology was investigated by ex situ atomic force microscopy (NT-MDT Solver P-47, Silicon tip). Cross-TEM microscopy was performed using a JEOL (JEM-2100F) field emission transmission electron microscope (TEM) operating at 200 KV. The measured samples were prepared by using a JEOL (JIB-4601F) focused ion beam (FIB) system.

^{59}*Co Zero-Field NMR Characterization*: FNR was performed by using a home-assembled phase coherent NMR spectrometer[46] and an untuned probe circuit, consisting of a four-turn flat sample coil made of thin copper strip terminated onto a 50 ohm resistor, producing its rf field in the film plane. The probe head and the sample were cooled at 77 K by immersion in liquid N_2. Spectra were recorded by exciting nuclear spin echoes at discrete frequencies by means of an equal-pulse spin-echo sequence, with pulse duration of 0.4 µs, delay between pulses of 2.75 µs, and repetition delay of 500 µs. The spectral amplitude was determined at each frequency point from the discrete Fourier transform of the echo signal, divided by frequency-dependent sensitivity $\propto \omega^2$. For each sample, the experimental parameters were kept fixed, except rf power and frequency which were scanned.

L-MOKE Characterization: Hysteresis loops were measured with the samples placed on a cold finger and in high vacuum conditions (pressure of $\approx 10^{-6}$ mbar). Light source: He-Ne laser source ($\lambda = 638.2$ nm). Applied H field was applied in the film plane, along the same direction of the rf field used. Note that both sample environments in FNR and MOKE setups are inert and should not result in any alteration of the properties of the samples.

Acknowledgements

M. Benini, A. Surpi, A. Riminucci, V. A. Dediu and I. Bergenti acknowledge the support of the EC projects INTERFAST (H2020-FET-OPEN-965046) and SINFONIA (H2020-FET-OPEN-964396). Stimulating and fruitful discussions with Prof. R, De Renzi, Dr. V. Kabanov, and Dr. A. Shumilin are gratefully acknowledged. The authors would like to acknowledge the invaluable technical help received from Mr. Federico Bona.

Open Access Funding provided by Consiglio Nazionale delle Ricerche within the CRUI-CARE Agreement.

Conflict of Interest

The authors declare no conflict of interest.

Data Availability Statement

The data that support the findings of this study are available from the corresponding author upon reasonable request.

Keywords

C_{60}, cobalt, Gaq_3, solid-state nuclear magnetic resonance (NMR), spinterfaces

Received: June 22, 2022
Revised: August 22, 2022
Published online:

[1] M. Cinchetti, V. A. Dediu, L. E. Hueso, *Nat. Mater.* **2017**, *16*, 507.
[2] C. Barraud, P. Seneor, R. Mattana, S. Fusil, K. Bouzehouane, C. Deranlot, P. Graziosi, L. Hueso, I. Bergenti, V. Dediu, F. Petroff, A. Fert, *Nat. Phys.* **2010**, *6*, 615.
[3] S. Sanvito, *Nat. Phys.* **2010**, *6*, 562.
[4] S. Steil, N. Großmann, M. Laux, A. Ruffing, D. Steil, M. Wiesenmayer, S. Mathias, O. L. A. Monti, M. Cinchetti, M. Aeschlimann, *Nat. Phys.* **2013**, *9*, 242.
[5] V. A. Dediu, *Nat. Phys.* **2013**, *9*, 210.
[6] S. Delprat, M. Galbiati, S. Tatay, B. Quinard, C. Barraud, F. Petroff, P. Seneor, R. Mattana, *J. Phys. D: Appl. Phys.* **2018**, *51*, 473001.
[7] S. Javaid, M. Bowen, S. Boukari, L. Joly, J.-B. Beaufrand, X. Chen, Y. J. Dappe, F. Scheurer, J.-P. Kappler, J. Arabski, W. Wulfhekel, M. Alouani, E. Beaurepaire, *Phys. Rev. Lett.* **2010**, *105*, 077201.
[8] A. Droghetti, P. Thielen, I. Rungger, N. Haag, N. Grossmann, J. Stockl, B. Stadtmuller, M. Aeschlimann, S. Sanvito, M. Cinchetti, *Nat. Commun.* **2016**, *7*, 9.
[9] S. Braun, W. R. Salaneck, M. Fahlman, *Adv. Mater.* **2009**, *21*, 1450.
[10] T. L. A. Tran, P. K. J. Wong, M. P. de Jong, W. G. van der Wiel, Y. Q. Zhan, M. Fahlman, *Appl. Phys. Lett.* **2011**, *98*, 222505.
[11] T. L. A. Tran, D. Çakır, P. K. J. Wong, A. B. Preobrajenski, G. Brocks, W. G. van der Wiel, M. P. de Jong, *ACS Appl. Mater. Interfaces* **2013**, *5*, 837.
[12] K. V. Raman, A. M. Kamerbeek, A. Mukherjee, N. Atodiresei, T. K. Sen, P. Lazić, V. Caciuc, R. Michel, D. Stalke, S. K. Mandal, S. Blügel, M. Münzenberg, J. S. Moodera, *Nature* **2013**, *493*, 509.
[13] T. Moorsom, M. Wheeler, T. M. Khan, F. Al Ma'Mari, C. Kinane, S. Langridge, D. Ciudad, A. Bedoya-Pinto, L. Hueso, G. Teobaldi, V. K. Lazarov, D. Gilks, G. Burnell, B. J. Hickey, O. Cespedes, *Phys. Rev. B* **2014**, *90*, 6.
[14] K. Bairagi, A. Bellec, V. Repain, C. Chacon, Y. Girard, Y. Garreau, J. Lagoute, S. Rousset, R. Breitwieser, Y.-C. Hu, Y. C. Chao, W. W. Pai, D. Li, A. Smogunov, C. Barreteau, *Phys. Rev. Lett.* **2015**, *114*, 5.
[15] K. Bairagi, A. Bellec, V. Repain, C. Fourmental, C. Chacon, Y. Girard, J. Lagoute, S. Rousset, L. L.e Laurent, A. Smogunov, C. Barreteau, *Phys. Rev. B* **2018**, *98*, 085432.
[16] M. Gruber, F. Ibrahim, S. Boukari, H. Isshiki, L. Joly, M. Peter, M. Studniarek, V. Da Costa, H. Jabbar, V. Davesne, U. Halisdemir, J. Chen, J. Arabski, E. Otero, F. Choueikani, K. Chen, P. Ohresser, W. Wulfhekel, F. Scheurer, W. Weber, M. Alouani, E. Beaurepaire, M. Bowen, *Nature Mater* **2015**, *14*, 981.
[17] T. Moorsom, S. Alghamdi, S. Stansill, E. Poli, G. Teobaldi, M. Beg, H. Fangohr, M. Rogers, Z. Aslam, M. Ali, B. J. Hickey, O. Cespedes, *Phys. Rev. B* **2020**, *101*, 060408.

[18] F. Al Ma'Mari, T. Moorsom, G. Teobaldi, W. Deacon, T. Prokscha, H. Luetkens, S. Lee, G. E. Sterbinsky, D. A. Arena, D. A. MacLaren, M. Flokstra, M. Ali, M. C. Wheeler, G. Burnell, B. J. Hickey, O. Cespedes, *Nature* **2015**, *524*, 69.
[19] C. Meny, P. Panissod, in *Annual Reports on NMR Spectroscopy* (Ed.: G. A. Webb), Academic Press, London, UK **2021**, pp. 47–96.
[20] A. C. Gossard, A. M. Portis, *Phys. Rev. Lett. 8*, *3*, 164.
[21] P. Panissod, *Structural and Magnetic Investigations of Ferromagnets by NMR. Application to Magnetic Metallic Multilayers*, Springer, Dordrecht, **1998**.
[22] H. A. M. de Gronckel, *The Nanostructure of Multilayered Films : A NMR Study*, Technische Universiteit Eindhoven, Eindhoven, NL **1993**.
[23] T. P. Das, *Phys. Scr.* **1975**, *11*, 121.
[24] P. Panissod, J. P. Jay, C. Meny, M. Wojcik, E. Jedryka, *Hyperfine Interact.* **1996**, *97*, 75.
[25] J. Lu, P. L. Kuhns, M. J. R. Hoch, W. G. Moulton, A. P. Reyes, *Phys. Rev. B* **2005**, *72*, 054401.
[26] M. Malinowska, M. Wojcik, S. Nadolski, E. Jedryka, C. Meny, P. Panissod, M. Knobell, A. D. C. Viegas, J. E. Schmidt, *J. Magn. Magn. Mater.* **1999**, *198–199*, 599.
[27] G. Avedissian, J. Arabski, J. A. Wytko, J. Weiss, C. Meny, *Phys. Rev. B* **2020**, *102*, 184114.
[28] G. Avedissian, J. Arabski, J. A. Wytko, J. Weiss, C. Meny, *Adv. Funct. Mater.* **2020**, *30*, 2005605.
[29] H. M. Hwang, J. Y. Park, S. K. Jung, J. Lee, C. N. Whang, S.-P. Kim, S.-C. Lee, K.-R. Lee, Y.-C. Chung, *J. Appl. Phys.* **2007**, *101*, 093525.
[30] J. D. R. Buchanan, T. P. A. Hase, B. K. Tanner, P. J. Chen, L. Gan, C. J. Powell, W. F. Egelhoff, *J. Appl. Phys.* **2003**, *93*, 8044.
[31] L. Gan, R. Gomez, C. J. Powell, R. McMichael, P. J. Chen, W. EgelhoffJr, *J. Appl. Phys.* **2003**, *93*, 8731.
[32] P. Panissod, C. Mény, *Appl. Magn. Reson.* **2000**, *19*, 447.
[33] R. Pang, X. Shi, M. A. Van Hove, *J. Am. Chem. Soc.* **2016**, *138*, 4029.
[34] C. Fourmental, L. L.e Laurent, V. Repain, C. Chacon, Y. Girard, J. Lagoute, S. Rousset, A. Coati, Y. Garreau, A. Resta, A. Vlad, C. Barreteau, A. Smogunov, D. Li, A. Bellec, *Phys. Rev. B* **2021**, *104*, 235413.
[35] R. Friedrich, V. Caciuc, N. S. Kiselev, N. Atodiresei, S. Blugel, *Phys. Rev. B* **2015**, *91*, 115432.
[36] C. Meny, in *Seventh Int. Conf. Thin Film Physics Applications* (Eds.: J. Chu, Z. Wang), Spie-Int Soc Optical Engineering, Bellingham, **2011**.
[37] C. Meny, E. Jedryka, P. Panissod, *J. Phys.: Condens. Matter* **1993**, *5*, 1547.
[38] W. F. Egelhoff, P. J. Chen, R. D. McMichael, C. J. Powell, R. D. Deslattes, F. G. Serpa, R. D. Gomez, *J. Appl. Phys.* **2001**, *89*, 5209.
[39] D. Li, C. Barreteau, S. L. Kawahara, J. Lagoute, C. Chacon, Y. Girard, S. Rousset, V. Repain, A. Smogunov, *Phys. Rev. B* **2016**, *93*, 085425.
[40] A. Droghetti, S. Steil, N. Grossmann, N. Haag, H. T. Zhang, M. Willis, W. P. Gillin, A. J. Drew, M. Aeschlimann, S. Sanvito, M. Cinchetti, *Phys. Rev. B* **2014**, *89*, 10.
[41] C. H. Lin, K. C. Lin, T. B. Tang, W. W. Pai, *J. Nanosci. Nanotechnol.* **2008**, *8*, 602.
[42] M. Callsen, V. Caciuc, N. Kiselev, N. Atodiresei, S. Blügel, *Phys. Rev. Lett.* **2013**, *111*, 106805.
[43] P. Bruno, *Phys. Rev. B* **1989**, *39*, 865.
[44] G. Bertotti, in *Hysteresis in Magnetism*, Academic Press, San Diego, **1998**, pp. 517–518.
[45] H. Ebert, *J. Phys.: Condens. Matter* **1989**, *1*, 9111.
[46] G. Allodi, A. Banderini, R. De Renzi, C. Vignali, *Rev. Sci. Instrum.* **2005**, *76*, 083911.